Coherence-multiplexed, label-free biomolecular interaction analysis

Sajal Chirvi,[1] Zexuan Qiang,[1] and Digant P. Davé[1,2,*]

[1]*Department of Bioengineering, University of Texas, Arlington, Texas 76010, USA*

[2]*Advanced Imaging Research Center, University of Texas Southwestern Medical Center, Dallas, Texas 75903, USA*

**Corresponding author: ddave@uta.edu*

Received January 9, 2012; revised May 8, 2012; accepted May 22, 2012;
posted May 23, 2012 (Doc. ID 160591); published July 13, 2012

This Letter describes an interferometric technique based on the principle of coherence multiplexing for multichannel, label-free biosensing applications. Multiple biosensors can be interrogated simultaneously with a single spectral-domain, phase-sensitive interferometer by coding the individual sensograms in coherence-multiplexed channels. The experimental results demonstrate the multiplexed quantitative biomolecular interaction of antibodies binding to antigen-coated functionalized biosensor chip surfaces. The described technique also applies to a variety of other distributed and multiplexed sensing applications besides biosensing.

OCIS codes: 280.1415, 120.3180, 120.0280, 060.2370, 030.1640.

Label-free optical techniques have emerged as potential alternatives to traditionally used label-based methods for numerous biosensing applications. Label-free biosensing has significant advantages such as lack of interference from labels, higher accuracy, and less expensive assays. Biomolecular interaction analysis (BIA) is a biosensing application where surface plasmon resonance (SPR), a label-free optical method, is now well established as a preferred technique for quantifying binding kinetics [1–2]. Instruments based on SPR for BIA are now commercially available and widely used in research and commercial applications. Exploiting the capability of SPR to detect ultrasmall changes in refractive index (RI), binding of biomolecules to functionalized biosensors chips is measured and quantified. Although SPR is a highly sensitive technique, it is not well suited for the highly multiplexed BIA required in high-throughput applications and implementation on many biosensing platforms.

Optical methods for label-free biosensing either measure change in the RI or optical path length (OPL), which occurs when target biomolecules bind to capture biomolecules on surface-functionalized biosensor chips. In the past decade, a number of label-free optical techniques have emerged in attempts to not only address limitations of SPR but also expand the range of biosensing applications. These techniques include reflectance interference spectroscopy [3–5], resonant waveguide sensing [5], photonic crystal sensing [6], and interferometry [7–9].

Recently, implementation of spectral-domain, phase-sensitive interferometry (SD-PSI) for label-free detection of biomolecules has been demonstrated [7–9]. One advantage of SD-PSI compared to other label-free techniques is that it does not require use of custom-fabricated biosensor substrates. Laboratory-grade, off-the-shelf glass or plastic substrate of suitable thickness with proper surface functionalization can be used as biosensor chips. Processes and protocols for surface modifications of glass and plastic substrates are well established for fabrication of molecular-tailored biosensor chips. Also, fiber-based SD-PSI is well suited for *in situ* and spatially distributed remote biosensing applications.

In this Letter, we demonstrate proof-of-principle implementation of coherence multiplexing for quantitative multichannel label-free biosensing using a fiber-based SD-PSI instrument. Coherence multiplexing permits simultaneous biosensing in multiple channels with a fiber-based instrument, which is a key advantage compared to other multiplexing techniques such as time division multiplexing. Figure 1 shows the basic concept and implementation of an N channel coherence-multiplexed, label-free biosensing using a phase-sensitive, SD interferometric setup.

Each channel for label-free biosensing in this configuration is a coherence-separated interference channel, in which the biosensor signal is encoded in a specific carrier frequency (spectral fringe frequency) that is determined by the optical thickness of the biosensor substrate. The interferometric setup consists of a low-coherence light source, single-mode fiber splitter ($1 \times N$), sensor substrates, and a high-resolution spectrometer. Light from a superluminescent diode ($\lambda_c = 800$ nm, $\Delta\lambda = 20$ nm) is seeded into the input port of the splitter after which it travels along each output branch (port) and is incident on individual biosensors. Light reflecting from the bottom (air–glass) and top (functionalized layer–buffer) interfaces of the biosensor substrate couples back into their respective fiber ports and superposes to generate spectral interference signals that are detected by the spectrometer. Essentially, each output fiber splitter branch along with the biosensor substrate constitutes an independent common-path interferometer. The spectral fringe frequency of the interferometric signal formed in each interferometric path is different due to the distinct thickness of each biosensor substrate. The combined spectral interferometric fringe signal (second panel, Fig. 1) from N biosensors and common-path interferometers detected by the spectrometer is given by the expression

$$S(k) = \alpha S_0(k)\left\{R_r + R_s + \sqrt{R_r R_s}|\mu(k)| \sum_{m=1}^{N} \cos(4\pi\Delta p_m k)\right\}, \tag{1}$$

where $S_0(k)$ is the incident spectral intensity; R_r and R_s are reference and sample surfaces, respectively,

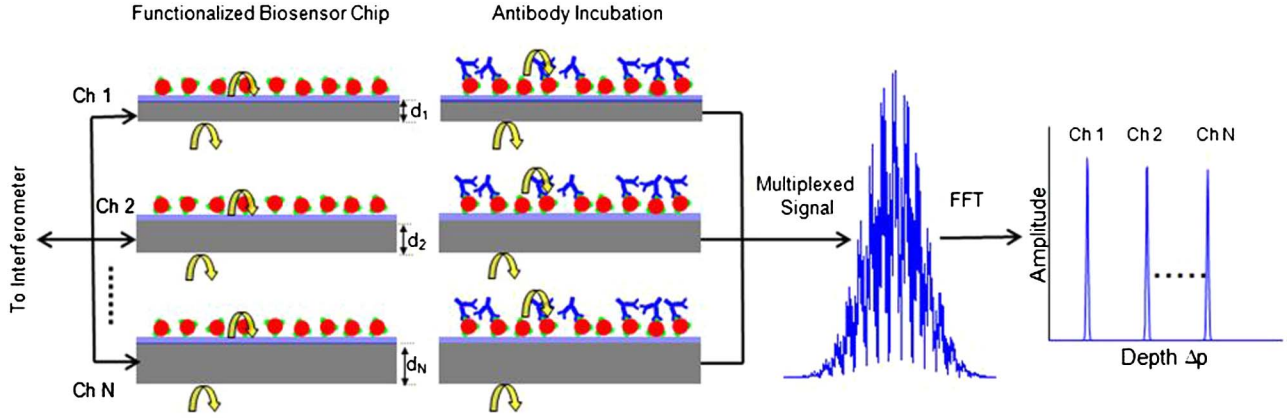

Fig. 1. (Color online) Schematic diagram showing the implementation of N channel coherence-multiplexed biosensing setup with a multichannel spectral domain interferometer. Each biosensor chip is attached to a separate output port of the interferometer. Fourier transform of the multiplexed spectral interference signal (middle panel) separates the signal in different channels (right panel).

responsible for generating the common-path interferometric spectral fringe signal; $\mu(k)$ is the spectral degree of coherence; Δp_m is the OPL ($= RI \times d_m$) difference between two surfaces of the mth biosensor; k is the optical wavenumber; and α is the fraction of seeded spectral light intensity coupled to each output branch of fiber splitter.

Biosensing information in each channel is obtained by Fourier transformation of Eq. (1), which indexes magnitude and phase of the interferometric signal as a function of OPL. Assuming a Gaussian line shape of the light source, Fourier transformation of Eq. (1) yields a Gaussian function with the peak centered at the mth spatial frequency index, where line width is proportional to the bandwidth of the light source. The maximum biosensing channel capacity of the coherence-multiplexed interferometer is a function of light source bandwidth and spectral resolution of the spectrometer and can be estimated by

$$N_{\max} = \frac{\Delta\lambda}{2\delta\lambda} = \frac{(\mathrm{OPL})_{\max}}{l_c}, \tag{2}$$

where $\Delta\lambda$ is the bandwidth of the light source, $\delta\lambda$ is the spectral resolution of the spectrometer, and l_c is the coherence length of the light source. The described interferometer has a maximum channel capacity of 100. Biomolecule binding sensitivity is a function of interferometer SNR. Higher OPL channels have reduced SNR due to reduction in modulation depth of spectral fringe signal. Binding of target biomolecules to the functionalized layer of the biosensor surface causes subwavelength OPL changes resulting in phase shift of the spectral interference fringe as function of time, which is used to plot the sensogram (OPL versus time). The phase shift in the mth sensor can be calculated by the expression

$$\varphi_m(t) = \tan^{-1}\left\{\frac{\mathrm{Im}\,\Im[S(k)]}{\mathrm{Re}\,\Im[S(k)]}\right\}\Bigg|_{z=\Delta p_m} = \frac{4\pi\Delta p_m}{\lambda_c}. \tag{3}$$

Proof-of-principle experiments to demonstrate coherence-multiplexed BIA were performed with a four-channel interferometer. Light exiting each fiber port was first collimated and then focused with a microscope objective lens to a functionalized sensor surface for interrogation. A custom-made microfluidic flow cell (Fig. 2) platform and multiwell plate platform were used for quantitative BIA experiments. In the flow cell platform, the biosensor chip is sandwiched between two aluminum plates and a sealing gasket. The top plate has an optical window through which the light is incident on the biosensor chip whereas the bottom plate has machined microfluidic channels and ports for entry and exit of fluid.

A multichannel peristaltic pump and a multiport injection valve connected in series with flow cells are used to transport selective fluid (buffer and biomolecules) to various biosensor chips. In the multiwell plate platform, a polydimethylsiloxane (PDMS) stamp with multiple punched holes of (100 μl well capacity) is bonded to a biosensor chip. The biosensor chips used for experiments are commercially available protein-capture microscope glass cover slips (CS) (Xenopore, Inc.) of various thicknesses (#1, #1.5, and #2, corresponding to the OPL of 190,

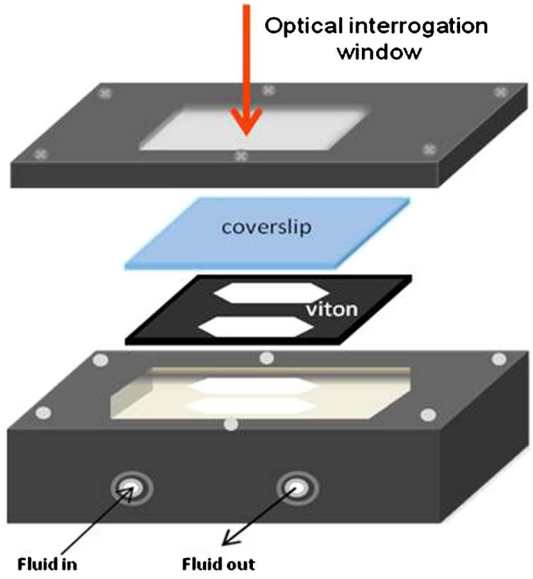

Fig. 2. (Color online) Microfluidic flow cell used to perform the multichannel BIA experiments.

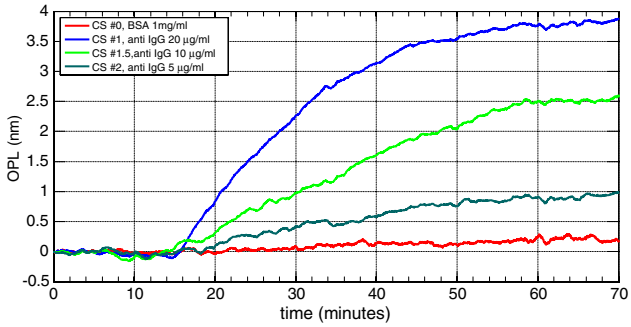

Fig. 3. (Color online) Sensogram plots of four-channel coherence-multiplexed BIA of anti-IgG and BSA binding to functionalized biosensors chips.

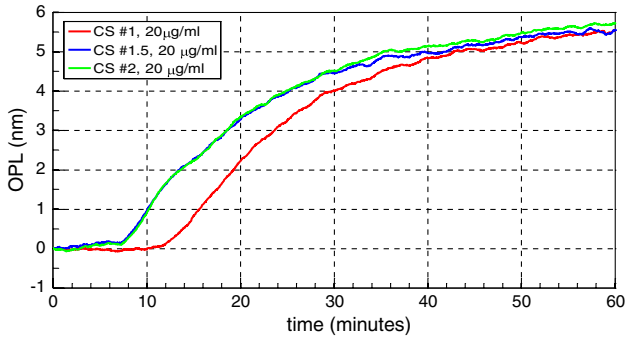

Fig. 4. (Color online) BIA of same concentration of anti-IgG binding to IgG functionalized in three different biosensing channels showing channel-to-channel reproducibility.

285, and 381 μm, respectively). The aldehyde groups on the surface of the CS spontaneously react with primary and secondary amine groups to create a covalent bond. The biosensor chips were functionalized with IgG (antigen) to capture anti-IgG (antibody) molecules. Additionally, a poly-D lysine coated #0 coverslip (OPL of 95 μm) was used for the experiments to have a total of four biosensing channels.

Multichannel sensograms recorded for anti-IgG binding to IgG are shown in Figs. 3 and 4. For all experiments, a baseline is first recorded for 5–15 min to establish stability by a flowing PBS buffer solution, which is followed by injection of anti-IgG or BSA solution for 45–50 min. The multiplexed spectral interference fringe signal detected by the line scan camera in the spectrometer is acquired at a 20 Hz rate, digitized, and transferred to the computer for storage and postprocessing. A software module written in LabView was used for spectral data acquisition, processing, and displaying the sensogram in real time. OPL in the sensograms is calculated using Eq. (3) assuming a RI of 1.5 for the binding protein (anti-IgG and BSA). The baseline φ_m value is arbitrary and is referenced to zero. In the sensogram plots, the calculated values of OPL change are with respect to the baseline. Raw sensograms were processed with a moving average filter to eliminate high-frequency phase noise. The spectral-domain interferometric setup used for the experiments has a single-channel phase noise (variance) of 1 mrad^2(= 63 pm^2), which determines the biomolecule detection sensitivity. For the IgG antibody, the detection sensitivity is 45 pg/mm^2. It should be noted that detection sensitivity depends on the size and RI of the biomolecule since the parameter being measured is OPL. Plotted sensograms are typical biomolecular binding curves, where the binding rate is proportional to the concentration of the binding target molecule, binding affinity, and density of capture sites on the functionalized biosensor chip surface. After initial sustained rise post biomolecule incubation, the binding curves asymptotically level off to a constant value proportional to their concentration. The binding curves differ in the flow and well platforms due to the difference in the fluidic environment (i.e., dynamic versus static).

Binding curves for various concentrations of anti-IgG (IgG antibodies) binding to IgG layer in a four well-plate platform are shown in Fig. 3. Also shown is binding of BSA to poly-D-lysine as an additional BIA channel. The rate of change and total change in OPL is proportional to the concentration of anti-IgG. Channel-to-channel repeatability is demonstrated by recording binding of same concentration of anti-IgG to IgG in different biosensing channels (Fig. 4).

In summary, a new method for simultaneous quantitative detection of biomolecular interaction in multiple channels with a single interferometer has been introduced. The methodology is well suited for high-throughput BIA applications, such as drug screening, where large libraries of candidate biomolecules have to be tested for biomolecular interactions. Fiber-based implementation and use of glass or plastic substrates as biosensors chip provides an additional advantage of applicability to a wider variety of multichannel biosensing applications and platforms. Direct attachment of biosensors chip to fiber tips will further expand the biosensing application range. The technique is vulnerable to fluctuation in temperature that will result in OPL change of the biosensors chip. Maintaining biosensor chips and buffer solutions at a constant temperature can minimize environmental temperature drifts. The technique will also be useful in other sensing applications such as multichannel distributed temperature and pressure sensor systems.

This work was supported by grants from the National Institutes of Health (EB008509), the Department of Energy (DE-FG02-O4CH11280), and Texas Ignition Funds.

References

1. J. Homola, Anal. Bioanal. Chem. **377**, 528 (2003).
2. A. Szabo, L. Stolz, and R. Granzow, Curr. Opin. Struct. Biol. **5**, 699 (1995).
3. O. Birkert, R. Tünnemann, G. Jung, and G. Gauglitz, Anal. Chem. **74**, 834 (2002).
4. J. Concepcion, K. Witte, C. Wartchow, S. Choo, D. Yao, H. Persson, W. Henrik, L. Jing, P. Li, B. Heidecker, W. Ma, R. Varma, L. Zhao, D. Perillat, G. Carricato, M. Recknor, K. Du, H. Ho, T. Ellis, J. Gamez, M. Howes, J. Phi-Wilson, S. Lockard, R. Zuk, and H. Tan, Comb. Chem. HTS **12**, 791 (2009).
5. Y. Fang, A. M. Ferrie, and E. Tran, Methods Mol. Biol. **552**, 239 (2009).
6. B. T. Cunningham and L. Laing, Expert Rev. Proteomics **3**, 271 (2006).
7. C. Joo, E. E. Ozkumur, M. Unlu, and J. Boer, Biosens. Bioelectron. **25**, 275 (2009).
8. C. Joo and J. F. de Boer, Opt. Lett. **32**, 2426 (2007).
9. D. P. Davé, Methods Mol. Biol. **503**, 179 (2009).